

**Ion-DMPS**

L. Laakso et al.

# Detecting charging state of ultra-fine particles: instrumental development and ambient measurements

L. Laakso<sup>1</sup>, S. Gagné<sup>1</sup>, T. Petäjä<sup>1</sup>, A. Hirsikko<sup>1</sup>, P. P. Aalto<sup>1</sup>, M. Kulmala<sup>1</sup>, and V.-M. Kerminen<sup>2</sup>

<sup>1</sup>Department of Physical Sciences, P.O. Box 64, 00014, University of Helsinki, Finland

<sup>2</sup>Finnish Meteorological Institute, Air Quality Research, P.O. BOX 503, 00101 Helsinki, Finland

Received: 25 April 2006 – Accepted: 4 May 2006 – Published: 13 July 2006

Correspondence to: L. Laakso (lauri.laakso@iki.fi)

Title Page

Abstract

Introduction

Conclusions

References

Tables

Figures

◀

▶

◀

▶

Back

Close

Full Screen / Esc

Printer-friendly Version

Interactive Discussion

EGU

## Abstract

The importance of ion-induced nucleation in the lower atmosphere has been discussed for a long time. In this article we describe a new instrumental setup – Ion-DMPS – which can be used to detect contribution of ion-induced nucleation on atmospheric new particle formation events. We performed several laboratory tests to test the operation of the device and then we measured atmospheric new particle formation events with the instrument in a boreal forest. We found that some of the events were clearly dominated by neutral nucleation but in some cases also ion-induced nucleation contributed to the new particle formation. We also found that negative and positive ions behaved in a different manner, days with negative overcharging were more frequent than days with positive overcharging. A simple order of magnitude estimate gave the contribution of ion-induced nucleation on total nucleation approximately 10%. During the neutral-dominated nucleation days ion contribution was close to zero.

## 1 Introduction

New particle formation is taking frequently place in the global atmosphere worldwide (Kulmala et al., 2004). Despite many observations, however, the exact nucleation mechanisms still remain an open question. Several nucleation pathways including ion-induced, ternary, binary and kinetic nucleation had been proposed, but the relative importance of these processes in different environments is still unknown. Ternary and binary nucleation refer to the number of vapors participating in the nucleation process, whereas ion-induced nucleation refers to the presence of charges in nucleation (Weber et al., 1996; Laakso et al., 2002). Thus, both binary and ternary nucleation can be either ion-induced or neutral. A recently-proposed particle nucleation mechanism is the activation of stable clusters (Kulmala et al., 2000, 2006), which can be either neutral or ion clusters (Kulmala et al., 2000).

Most studies on atmospheric nucleation are based on utilization of electric charges

ACPD

6, 6401–6429, 2006

**Ion-DMPS**

L. Laakso et al.

Title Page

Abstract

Introduction

Conclusions

References

Tables

Figures

◀

▶

◀

▶

Back

Close

Full Screen / Esc

Printer-friendly Version

Interactive Discussion

EGU

and electric fields (for an overview, see e.g. [Flagan, 1998](#)). Such devices include ion mass spectrometers, ion-spectrometers and Differential Mobility Particle Sizer (DMPS) ([Aalto et al., 2001](#); [Weber et al., 1995](#); [Winklmayr et al., 1991](#)). Ion mass spectrometers have been used successfully in the studies of new particle formation in the upper atmosphere ([Eichkorn et al., 2002](#)). Recent developments in atmospheric measurements are the ion spectrometers which detect ion or charged aerosol distributions from cluster ion sizes up to the Aitken mode ([Laakso et al., 2004](#)). Typically, ion spectrometers measure both polarities.

The most common aerosol sampling instrument utilizing an electric field is the Differential Mobility Analyzer (DMA) in a DMPS-system. In the DMA aerosol particles of certain mobility are chosen from an air flow. In the DMPS system, only the charged fraction of particles is measured. The equilibrium charge on particles is provided by a radioactive bipolar or by a unipolar corona charger. The total particle number concentration is obtained after a mathematical inversion of the charged fraction. Since only few percent of particles in small sizes are charged, this inversion procedure is very sensitive to understanding the charging probability of particles.

The charged fraction can be calculated from different theories, most widely-used are the semi-empirical theories by [Hoppel and Frick \(1986\)](#) and [Wiedensohler \(1988\)](#) as well as the flux-matching theory by [Fuchs and Sutugin \(1970\)](#).

Unfortunately, despite numerous laboratory studies, the particle charging probability in the atmosphere is not well-known, especially for the smallest particle sizes ([Reischl et al., 1996](#)). Thus, if we are interested in freshly-formed nanoparticles, more information on atmospheric charging probabilities is needed ([Hussin et al., 1983](#); [Reischl et al., 1996](#)).

In addition to being necessary for interpreting instrumental results, electric charges may also carry information about the nucleation processes. In case of ion-induced nucleation, new particles are formed electrically charged, whereas in case of neutral nucleation particles do not initially carry any charges. Thus, depending on nucleation mechanism, the charging state of particles may deviate from that in the charge equi-

## Ion-DMPS

L. Laakso et al.

Title Page

Abstract

Introduction

Conclusions

References

Tables

Figures

◀

▶

◀

▶

Back

Close

Full Screen / Esc

Printer-friendly Version

Interactive Discussion

librium. When nucleated particles grow, they will finally reach the electrical equilibrium (Vana et al., 2005). In this study, we use the term charging probability when referring to the fraction of charged particles in the equilibrium state. The term charged fraction tells how large is the percentage of charged particles at a certain size. The term charging state refers to the charged fraction with respect to the charged fraction in the equilibrium state (charging probability). If there are fewer charged particles than there would be in the equilibrium state, the charging state of the particles is undercharged. If the number of charged particles exceeds the equilibrium value, the particles are overcharged.

In this work, we present a new instrumental setup which can be used to define charging state of aerosol particles. A preliminary version of this device was utilized already by Mäkelä et al. (2003) but the results remained unpublished. After describing the instrument and its measurement principles, we present a laboratory verification of the instrument. Then we apply the instrument to ambient new particle formation events. Finally, the results and their consequences are discussed.

## 2 Instrumentation

### 2.1 Ion-DMPS

The ion-Differential Mobility Particle Sizer (ion-DMPS) is based on a well-defined aerosol sizing instrumentation concentrating on the ultra-fine particle size range (<15 nm in diameter (Aalto et al., 2001). A schematic picture of the instrument is presented in Fig. 1 (boxed with dashed line). First, aerosol particles are led to a bipolar charger (Ni-63) that can be switched on and off. Next, they are led through a conventional Differential Mobility Analyzer (DMA, length 0.109 m, (Winklmayr et al., 1991) with a switchable two-polarity high voltage power supply. By changing the polarity in the DMA, we were able to measure either positive or negative particles. The DMA was operated with a closed loop flow (Jokinen and Mäkelä, 1997). The size segregated par-

Title Page

Abstract

Introduction

Conclusions

References

Tables

Figures

◀

▶

◀

▶

Back

Close

Full Screen / Esc

Printer-friendly Version

Interactive Discussion

ticles were detected with a TSI 3025 (Stolzenburg and McMurry, 1991) ultrafine particle counter (CPC). Given the maximum voltage, flow rates, and counting efficiency of the CPC, this corresponded to a size range approximately from 3 to 15 nm in electrical mobility equivalent diameter.

Small adjustments to this kind of conventional instrument enabled us to measure aerosol particle size distribution in four different operating modes: 1) the charger was on and the DMA had a negative polarity; 2) the charger was off and the DMA had a negative polarity; 3) the charger was on and the DMA had a positive polarity; 4) the charger was off and the DMA had a positive polarity. For each operation mode, a size scan with pre-defined intervals was carried out.

### 2.1.1 Laboratory verification of Ion-DMPS

The ion-DMPS was tested in a laboratory prior to deployment under field conditions. Several tests were performed with monodisperse ammonium sulphate and silver particles. The laboratory setup is depicted in Fig. 1. Polydisperse ultrafine silver particles were generated with an oven (Carbolite Furnaces MTF 12/388). The equilibrium charge distribution was obtained with a bipolar NI-63 charger and from this generated particle population a monodisperse selection was extracted with a Vienna type Differential Mobility Analyser (DMA, length 0.109 m. The sheath flow was set to  $20 \text{ l min}^{-1}$  and aerosol flow to  $1 \text{ l min}^{-1}$ . The aerosol sample was then separated between the ion-DMPS and TSI model 3025 Ultrafine Condensation Particle (UCPC, Stolzenburg and McMurry, 1991), the latter of which was used as a reference instrument for absolute particle concentration. In addition, with the aid of the reference instrument, it was also possible to normalize small fluctuations in the aerosol generation system.

### 2.1.2 Transport efficiency

The purpose of the ion-DMPS is to determine the charging state of ultra-fine particles. Although knowing the absolute particle concentration is not essential in doing that, the

Title Page

Abstract

Introduction

Conclusions

References

Tables

Figures

◀

▶

◀

▶

Back

Close

Full Screen / Esc

Printer-friendly Version

Interactive Discussion

initial ultra-fine particle concentration has to be large enough to penetrate through the system and give a reliable concentration reading during the counting. The transport efficiency through the ion-DMPS was determined experimentally with monodisperse silver particles ranging from 3 to 40 nm in electrical mobility equivalent diameter. The transport efficiency was a steep exponential curve. Roughly 75% of 20 nm particles penetrated the setup, whereas only 25% of 5 nm particles survived. In the normal operation range of 3–15 nm, the transport efficiency of the setup is 15 to 65%. The cut-size, i.e. the diameter at which the transport efficiency is 50%, was 7.2 nm. This corresponds to a laminar flow diffusion loss ([Baron and Willeke, 2001](#)) of 16.4 m of a circular tube. The losses are, however, not as crucial to the performance of the ion-DMPS as they are in case of a normal size distribution instrument. In the ion-DMPS, the desired information is the ratio between the concentrations, which are exposed to the same losses despite their polarities or the number of charges.

### 2.1.3 Charge balance and neutralization efficiency

A charge balance of laboratory-generated particles was determined with the ion-DMPS for ammonium sulphate and silver particles (Fig. 2). All the ratios were normalized with respect to the concentration of negative, non-neutralized particles. As neutralized poly-disperse particles were sampled with the ion-DMPS, several features were detected. Firstly, switching on the charger increased the concentration of sub-10 nm particles by approximately 10% in comparison with corresponding non-neutralized negative particle concentration. This effect was more pronounced in the ammonium sulphate experiments. Absolute concentrations were higher in the case of negative polarity. This is due to higher mobilities of negative cluster ions, which attach to the sampled particles in the ion-DMPS charger. This has been seen in earlier experiments ([Wiedensohler, 1988](#)) as well as using theoretical calculations ([Fuchs and Sutugin, 1970](#); [Hoppel and Frick, 1986](#)). As the particle size decreases, the absolute charging efficiency decreases for both polarities. On the other hand, the ratio between the negative and positive charging efficiencies did not remain the same in our experiments. To clarify this, more laboratory

Title Page

Abstract

Introduction

Conclusions

References

Tables

Figures

◀

▶

◀

▶

Back

Close

Full Screen / Esc

Printer-friendly Version

Interactive Discussion

experiments are needed to experimentally determine the particle charging efficiency in the sub-10 nm size range.

A crucial part of the ion-DMPS is the radioactive charger in front of the instrument. Since our aim was to determine the charging state, i.e. the excess or deficit of electrical charges in ultra-fine particles, the radioactive source in the system has to be strong enough to efficiently neutralize the charging state of the sampled particles to equilibrium conditions. This is needed in the calculation of over / undercharging state as a reference concentration. To test this, higher than atmospheric concentrations of negatively charged silver particles utilizing the laboratory setup were generated. The ion-DMPS distributions measured with the charger and positive polarity (i.e. neutralized negative particles) agreed well with a parameterization by [Wiedensohler \(1988\)](#). This indicates that the charger was in working order.

## 2.2 Balanced Scanning Mobility Sizer (BSMA)

In addition to ion-DMPS, we carried out ion measurements using a Balanced Scanning Mobility Sizer (BSMA) ([Tammets, 2004, 2006](#)). The Balanced Scanning Mobility Analyzer, manufactured by Airel Ltd., Estonia, consists of two plain aspiration-type Differential Mobility Analyzers, one for positive and the other for negative ions. The two aspiration condensers are connected as a balanced bridge circuit that allows continuous variation of the driving voltage and scanning of the mobility distribution of charged clusters and nanoparticles. A large airflow rate 44 l per second helps to suppress the loss of air ions in the inlet of the instrument. The inlet can be closed or opened for ions using a controlled electrostatic filter and the background signal is eliminated by making every second scan with a closed inlet. A mobility distribution is calculated according to the results of 9 scans performed over 3 min. The electric mobility range of  $0.032\text{--}3.2\text{ cm}^2\text{V}^{-1}\text{s}^{-1}$  is logarithmically uniformly divided into 16 fractions. The corresponding size distribution is presented by 10 fractions, logarithmically equally distributed in a diameter range of 0.4–7.5 nm.

Title Page

Abstract

Introduction

Conclusions

References

Tables

Figures

◀

▶

◀

▶

Back

Close

Full Screen / Esc

Printer-friendly Version

Interactive Discussion

### 3 Data treatment and analysis

#### 3.1 Interpretation of ion-DMPS-results

Figure 4 represents schematically four different cases of nucleation and how they are observed by an ion-DMPS.

In case of neutral nucleation all particles are formed electrically neutral from nucleating vapors (Fig. 4, first row), whereas in ion-induced particle formation nucleation takes place on pre-existing cluster ions so that all freshly-formed particles carry one positive or negative elementary charge (Fig. 4, second row). When the particles grow bigger, they tend to reach charge equilibrium. In addition to pure neutral or ion-induced nucleation, different combinations of these two mechanisms are also possible. The third row in Fig. 4 represents the case where ion-induced nucleation dominates over neutral nucleation, whereas in the fourth row of Fig. 4 neutral nucleation dominates over ion-induced nucleation.

In addition to the cases presented in Fig. 4, it is also possible that positive and negative ions behave in a different way, i.e. ion-induced nucleation can have a charge preference (Kusaka et al., 1995; Lovejoy et al., 2004). For that reason we measured both the polarities. Common to all different nucleation combinations, the only way to receive an overcharging is that at least some fraction of the new particles have originated from ion-induced nucleation.

An example of inverted Ion-DMPS data together with conventional DMPS-data is shown in Fig. 5. The concentration of negative natural particles was higher during the first hour of the event than the corresponding concentrations after the ambient particles were neutralized with the radioactive source (Fig. 5c and d, respectively). In other words, fresh atmospheric particles during this day carried excess negative charges compared with the equilibrium state. This is an indication of the participation of ions in the first steps of the particle formation process. Also positive particles were slightly overcharged.

One way to analyze the possible existence of ion-induced nucleation is to calculate

Title Page

Abstract

Introduction

Conclusions

References

Tables

Figures

◀

▶

◀

▶

Back

Close

Full Screen / Esc

Printer-friendly Version

Interactive Discussion



the ratio between the natural to neutralized particle concentrations (right column in Fig. 4). If the ratio is  $>1$ , the particles are overcharged compared to the equilibrium state. On the other hand, if the ratio is  $<1$ , the particles are undercharged. The benefit in using this ratio and one single inlet lies in the fact that it allows us to avoid systematic errors due to losses within the inlet structure.

By dividing the natural ion concentration (only values over  $0.1 \text{ cm}^{-3}$  are used) by the neutralized ion concentration for each diameter and time, we obtain the charging state as a function of time and particle size. This state is averaged over the nucleation period for each diameter. Two example cases are shown in Figs. 6 and 7. In Fig. 6 (21 May 2005) one can observe an overcharged nucleation event for both positive and negative ions, whereas in Fig. 7 (2 May 2005) particles of both polarities are undercharged.

An example of the time behavior of the charging state is shown in Fig. 8. As shown in Fig. 8 the charging states of 5 and 7  $\mu\text{m}$  particles are pretty constant during the day. On the other hand the charging state of 3  $\mu\text{m}$  particles vary a lot from 7 to 1. It is also decreasing during the day indicating that ion clusters will first activate or ion induced nucleation are more important before noon than later.

## 4 Results from atmospheric measurements

We measured with our ion-DMPS at Hyytiälä Forestry field station (Vesala et al., 1998; Kulmala et al., 2001) during spring 2005 as a part of BACCI-QUEST intensive field campaign. The device was located in the main cottage of the station; the inlet was at 2 m height. We checked the ion-DMPS several times during the measurements by producing ammoniumsulphate aerosol which was first neutralized and then led to ion-DMPS. Then we sampled aerosol with charger on and off and compared the measured concentrations between these two states.

Title Page

Abstract

Introduction

Conclusions

References

Tables

Figures

◀

▶

◀

▶

Back

Close

Full Screen / Esc

Printer-friendly Version

Interactive Discussion

## 4.1 General features of nucleation mode charging state

The analysis was made for those days during which we were able to use data from ion-DMPS, BSMA and DMPS.

Figure 9 shows the charging state of different-size particles during all the event days observed, 34 days in total. One can see that negative ions tended to be overcharged for smaller diameters and close to equilibrium for bigger particles. The same tendency was observed for positive ions. However, for one day (2 May 2005, see also Fig. 7) the positive and the negative ions were undercharged at lower particle sizes reaching equilibrium at larger sizes. Compared with event days, the particle charging state seemed to behave quite differently during the five non-event days observed (Fig. 9). One must remember, however, that the charging state of sub-5 nm particles could not be determined during the non-event days due to absence of these particles from the measured size spectra.

Kerminen and Kulmala (2002) described a method for calculating the formation rate of 1-nm particles from the formation rate of 3 nm or larger particles by using observed particle growth rates and condensation sinks. If we repeat this calculation for charged particles, and make the following assumptions: 1) the ion-aerosol attachment coefficient between cluster ions and sub-10 nm particles is not size dependent, 2) all particles grow in size at a constant rate, 3) the cluster ion concentration does not change during the event and 4) self-coagulation of sub-10 nm particles is negligible, the charging state of different-size particles should follow the following equation:

$$C(d_p) = 1 + \beta \times \exp[-\lambda(d_p/d_0 - 3)] \quad (1)$$

Here,  $d_0$  is a non-dimensionalizing coefficient (1 nm), the parameter  $\beta$  gives the magnitude of the potential over/under charging and the parameter  $\lambda$  tells how rapidly particles reach the charge equilibrium when growing in size. Equation (1) can be used for two different purposes: to characterize the behavior and magnitude of the charging state on different days and to estimating the maximum contribution of ion-induced nucleation to new particle formation.

Title Page

Abstract

Introduction

Conclusions

References

Tables

Figures

◀

▶

◀

▶

Back

Close

Full Screen / Esc

Printer-friendly Version

Interactive Discussion

[Title Page](#)[Abstract](#)[Introduction](#)[Conclusions](#)[References](#)[Tables](#)[Figures](#)[◀](#)[▶](#)[◀](#)[▶](#)[Back](#)[Close](#)[Full Screen / Esc](#)[Printer-friendly Version](#)[Interactive Discussion](#)

Equation 1 was fitted to the measurement data by minimizing the distance between the experimental points (median particle number concentrations in different size ranges over the nucleation event) and the exponential function given by Eq. (1). Days with median particle number concentration remaining below  $0.1 \text{ cm}^{-3}$  in several size ranges were left out of the analysis. The fittings for all the 34 days are presented in Table 1.

When the parameter  $\beta > 0$  we have an overcharged state, whereas  $\beta < 0$  is indicative of an undercharged state. All  $\lambda$  parameters were positive, showing that the particle charging state tended to approach equilibrium when they grow in size. As visible in Table 1, there were many days during which the particle concentrations were too low to make a reliable fitting. This was the case especially for positive particles. It is also important to emphasize on the high sensibility of the fit especially when the number of points reaching the minimum concentration for smaller diameters is low. In such a case, the median for 3 nm can vary enough to change the  $\beta$  and  $\lambda$  parameters, but generally not the charging state.

## 4.2 Contribution of ion-induced nucleation to the total nucleation rate

If the four assumptions made in the previous subsection hold, i.e. the processes growing particles and carrying towards the charge equilibrium are similar between the size-ranges 1–3 nm and 3–15 nm, we may extrapolate the fitting given by Eq. (1) down to 1 nm. This gives us the particle charging state at 1 nm, from which we can then estimate the maximum contribution of ion-induced nucleation.

Table 1 shows that the calculated charging state of 1 nm particles varies a lot between the events, the median over charging being equal to 10 for negative charges and equal to 2.5 for positive charges. Since the charging probability of 1-nm particles is about 1%, we can estimate that the typical contribution of ion-induced nucleation was approximately 10% of the total nucleation rate during the observation period. However, this value might vary depending on the season; here we have used data from late spring only.

For a few days presented in Table 1 the calculated over charging at 1 nm is higher

than would be expected even if ion-induced nucleation contributed 100% of the total nucleation rate. This suggests that during these days, either our measurement uncertainties were too large to make a reliable fit into the measurement data, or the assumptions made in deriving Eq. (1) were not valid for extrapolation of the fitting curve into the size range 1–3 nm. In the following we discuss briefly the latter possibility and its consequences.

One of the main processes affecting the change of a particle population toward the charge equilibrium is ion-aerosol attachment. In the theory by Hoppel and Frick (1986) the attachment coefficients of opposite charges are almost constant over the size range 1–5 nm, whereas in the theory by Fuchs and Sutugin (1970) however, the attachment coefficient increases linearly with increasing particle size. If the theory by Fuchs and Sutugin (1970) were correct, i.e. the ion attachment would be less effective at smaller particle sizes compared with larger particle sizes, our approach would overestimate the contribution of ion-induced nucleation to the total nucleation rate.

The growth rates of 1–3 nm particles might be larger or smaller than those of >3 nm particles. The former might result from the possible effect of enhanced condensation growth of charged clusters (Yu and Turco, 2000), leading to overestimation of the contribution of ion-induced nucleation using our approach. Observations in Hyytiälä indicate, however, that the particle growth rate increases rather than decreases with increasing particle size, with typical particle growth rates being higher by a factor 2–3 at the 5 nm size compared with the 2 nm size (Hirsikko et al., 2005). If this is true, the real contribution of ion-induced nucleation could be approximately twice that obtained from our calculation.

Our assumption of constant cluster ion concentration does not significantly affect the results. Typically, variation during the event is less than 10%, and normally the concentration is decreasing rather than increasing. If the cluster ion concentration decreases, once again our method overestimates the contribution of ion-induced nucleation.

Self-coagulation of charged and neutral sub-5 nm particles starts to become important when the concentration of these particles exceeds about 100 000 particles per cc

## Ion-DMPS

L. Laakso et al.

Title Page

Abstract

Introduction

Conclusions

References

Tables

Figures

◀

▶

◀

▶

Back

Close

Full Screen / Esc

Printer-friendly Version

Interactive Discussion

(Kerminen and Kulmala, 2002). During our measurements the particle concentrations remained well below this limit, so the effect of self-coagulation on our results can be considered negligible.

In summary, the above uncertainty analysis indicates that we have overestimated rather than underestimated the contribution of ion-induced nucleation. If we take a direct estimation that using the fact that maximum contribution is 100%, we can then divide all ion induced fraction given in Table by a factor of 3. In that case the median value is around 3% for negative ions and around 1% for positive ion, and during most of the days. However, during 7 days the contribution is more than 10% and in one day it is 100%. The overall result is that ion induced nucleation (or activation of ion clusters) is not that significant way to form new aerosol particles than neutral nucleation. This is consistent with the recent observations by Eisele et al. (2006).

### 4.3 Comparison with BSMA measurements

We also compared our results from the Ion-DMPS with observations from the BSMA. This was done by calculating the average concentration over the nucleation period for each size and then fitting a line to the data points (see Fig. 10 and the first column in Fig. 4). We have then three different possibilities: 1) concentration of ions decreases (negative slope) 2) concentration of ions is constant (zero slope) 3) concentration of ions increases as a function of size (positive slope). We can now analyze these cases more in detail

- Case 1: We can obtain this situation with two different ways. If we have ion-induced nucleation, we have high concentration of ions at small sizes. When the particles grow bigger, charged particles get neutralized and their concentration decreases. In addition, concentration of charged particles decreases due to coagulation scavenging. However, another possibility for decreasing charged particle concentration is neutral nucleation. If we have high neutral nucleation rate, part of the particles are charged. Due to coagulation loss, number of all

Title Page

Abstract

Introduction

Conclusions

References

Tables

Figures

◀

▶

◀

▶

Back

Close

Full Screen / Esc

Printer-friendly Version

Interactive Discussion

[Title Page](#)[Abstract](#)[Introduction](#)[Conclusions](#)[References](#)[Tables](#)[Figures](#)[◀](#)[▶](#)[◀](#)[▶](#)[Back](#)[Close](#)[Full Screen / Esc](#)[Printer-friendly Version](#)[Interactive Discussion](#)

particles rapidly decreases, and despite increasing charging probability with increasing size, overall effect can be decreasing of charged particles as a function of size. Thus, in this case we can not say anything about nucleation mechanism.

- Case 2: Same arguments as in Case 1 apply and we can not say anything about the nucleation mechanism.
- Case 3: If the concentration of charged particles increases with increasing size, neutral nucleation have to dominate.

Figure 11 shows the slope of BSMA fittings vs.  $\beta$ . The results indicate that the days with high positive slope values particles are clearly less charged and thus neutral nucleation dominates.

## 5 Conclusions

In this study, we introduced a new DMPS setup which gives information on nucleation processes. We also showed experimental data from 34 new particle formation days from Hyytiälä. Some of the days were clearly overcharged which indicates contribution of ion-induced nucleation on new particle formation whereas some days were undercharged and thus neutral nucleation dominates. The behavior of negative ions differed from that of positive ones; there were usually more negative overcharging compared to positive overcharging. Our results clearly indicate that ion-induced nucleation take place in the atmosphere. The results also indicate that ion-induced nucleation has clear sign preference in favor of negative ions. Order of magnitude estimate gives a typical ion-induced nucleation contribution to the total nucleation rate during the period studied approximately 4%. Minimum contribution was found to be close to 0% and maximum close to 100%

In the future, we will utilize this experimental setup for calculating quantitatively the contribution of ion-induced nucleation on boreal new particle formation episodes for one full year of measurements.

## References

- Aalto, P., Hämeri, K., Becker, E., Weber, R., Salm, J., Mäkelä, J. M., Hoell, C., O'Dowd, C. D., Karlsson, H., Hansson, H.-C., Väkevä, M., Koponen, I. K., Buzorius, G., and Kulmala, M.: Physical characterization of aerosol particles during nucleation events, *Tellus*, 53B, 344–358, 2001. [6403](#), [6404](#)
- Baron, P. and Willeke, K.: *Aerosol Measurement: Principles, Techniques, and Applications*, 2nd edition, John Wiley and Sons, 2001. [6406](#)
- Eichkorn, S., Wilhelm, S., Aufmhoff, H., Wohlfrom, K., and Arnold, F.: Cosmic ray-induced aerosol formation: First evidence from aircraft-based ion mass spectrometer measurements, *Geophys. Res. Lett.*, 29, 14, 2002. [6403](#)
- Eisele, F. L., Lovejoy, E. R., Kosciuch, E., Moore, K., Mauldin III, R., Smith, J.-N., McMurry, P., and Iida, K.: Negative atmospheric ions and their potential role in ion-induced nucleation, *J. Geophys. Res.*, 111, D04305, doi:10.1029/2005JD00, 2006. [6413](#)
- Flagan, R.: History of Electrical Aerosol Measurements, *Aerosol Sci. Technol.*, 28, 301–380, 1998. [6403](#)
- Fuchs, N. A. and Sutugin, A. G.: *Highly dispersed aerosols.*, Ann Arbor Science Publishers, Ann Arbor, London, 1970. [6403](#), [6406](#), [6412](#)
- Hirsikko, A., Mordas, G., Aalto, P., Mirme, A., Hörrak, U., and Kulmala, M.: Calibration of the Air Ion Spectrometer, in *Research Unit on Physics, Chemistry and Biology of Atmospheric Composition and Climate Change: III Progress Report and Proceedings of Seminar in Pallas 29.3.–1.4.2005*, edited by: Kulmala, M. and Ruuskanen, T., no. 73 in *Report Series in Aerosol Science*, 87–90, 2005. [6412](#)
- Hoppel, W. and Frick, G.: Ion-aerosol attachment coefficients and steady-state charge distribution on aerosols in a bipolar environment, *Aerosol Sci. Technol.*, 5, 1–21, 1986. [6403](#), [6406](#), [6412](#)
- Hussin, A., Scheibel, H., Becker, K., and Porstendorfer, J.: Bipolar diffusion charging of aerosol particles – I: Experimental results within the diameter range 4–30 nm, *J. Aerosol Sci.*, 14, 671–677, 1983. [6403](#)
- Jokinen, V. and Mäkelä, J. M.: Closed loop arrangement with critical orifice for DMA sheath/excess flow system, *J. Aerosol Sci.*, 28, 643–648, 1997. [6404](#)
- Kerminen, V. M. and Kulmala, M.: Analytical formulae connecting the “real” and the “apparent” nucleation rate and the nuclei number concentration for atmospheric nucleation events, *J.*

Title Page

Abstract

Introduction

Conclusions

References

Tables

Figures

◀

▶

◀

▶

Back

Close

Full Screen / Esc

Printer-friendly Version

Interactive Discussion

## Ion-DMPS

L. Laakso et al.

[Title Page](#)[Abstract](#)[Introduction](#)[Conclusions](#)[References](#)[Tables](#)[Figures](#)[◀](#)[▶](#)[◀](#)[▶](#)[Back](#)[Close](#)[Full Screen / Esc](#)[Printer-friendly Version](#)[Interactive Discussion](#)

Aerosol Sci., 33, 609–622, 2002. [6410](#), [6413](#)

Kulmala, M., Pirjola, L., and Mäkelä, J. M.: Stable sulphate clusters as a source of new atmospheric particles, *Nature*, 404, 66–69, 2000. [6402](#)

5 Kulmala, M., Hämeri, K., Aalto, P., Mäkelä, J., Pirjola, L., Nilsson, E. D., Buzorius, G., Rannik, Ü., Dal Maso, M., Seidl, W., Hoffmann, T., Janson, R., Hansson, H.-C., Viisanen, Y., Laaksonen, A., and O'Dowd, C.: Overview of the international project on biogenic aerosol formation in the boreal forest (BIOFOR), *Tellus B*, 53, 324–343, 2001. [6409](#)

Kulmala, M., Vehkamäki, H., Petäjä, T., Dal Maso, M., Lauri, A., Kerminen, V.-M., Birmili, W., and McMurry, P.: Formation and growth rates of ultrafine atmospheric particles: a review of  
10 observations, *J. Aerosol Sci.*, 35, 143–176, 2004. [6402](#)

Kulmala, M., Lehtinen, K. E. J., and Laaksonen, A.: Cluster activation theory as an explanation of the linear dependence between formation rate of 3 nm particles and sulphuric acid concentration, *Atmos. Chem. Phys.*, 6, 787–793, 2006. [6402](#)

Kusaka, I., Wang, Z.-G., and Seinfeld, J. H.: Ion-induced nucleation, II, Polarizable multipolar molecules, *J. Chem. Phys.*, 103, 8993–9009, 1995. [6408](#)

15 Laakso, L., Mäkelä, J., Pirjola, L., and Kulmala, M.: Model studies on ion-induced nucleation in the atmosphere, *J. Geophys. Res.*, D(107), 4427, doi:10.1029/2002JD, 2002. [6402](#)

Laakso, L., Anttila, T., Lehtinen, K., Aalto, P., Kulmala, M., Hörrak, U., Paatero, J., Hanke, M., and Arnold, F.: Kinetic nucleation and ions in boreal particle formation events, *Atmos. Chem. Phys.*, 4, 2353–2366, 2004. [6403](#)

20 Lovejoy, E., Curtius, J., and Froyd, K.: Atmospheric ion-induced nucleation of sulfuric acid and water, *J. Geophys. Res.*, 109, D08204, doi:10.1029/2003JD004460, 2004. [6408](#)

Mäkelä, J. M., Salm, J., Smirnov, V. V., Koponen, I., Paatero, J., and Pronin, A. A.: Electrical charging state of fine and ultrafine particles in boreal forest air, *J. Aerosol Sci.*, 32, 149–150, 2003. [6404](#)

25 Reischl, G., Mäkelä, J., Karch, R., and Nécid, J.: Bipolar charging of ultrafine particles in the size range below 10 nm, *J. Aerosol Sci.*, 27, 931–949, 1996. [6403](#)

Stolzenburg, M. and McMurry, P.: An ultrafine aerosol condensation nucleus counter, *Aerosol Sci. Technol.*, 14, 48–65, 1991. [6405](#)

30 Tammet, H.: Balanced Scanning Mobility Analyzer, 16th International Conference on Nucleation & Atmospheric Aerosols (ICNAA) in Kyoto, 294–297 2004. [6407](#)

Tammet, H.: Continuous scanning of the mobility and size distribution of charged clusters and particles in atmospheric air and the Balanced Scanning Mobility Analyzer BSMA, *Atmos.*



## Ion-DMPS

L. Laakso et al.

[Title Page](#)[Abstract](#)[Introduction](#)[Conclusions](#)[References](#)[Tables](#)[Figures](#)[◀](#)[▶](#)[◀](#)[▶](#)[Back](#)[Close](#)[Full Screen / Esc](#)[Printer-friendly Version](#)[Interactive Discussion](#)

Res., accepted, 2006. [6407](#)

Vana, M., Tamm, E., Hörrak, U., Mirme, A., Tammet, H., Laakso, L., Aalto, P., and Kulmala, M.: Charging state of atmospheric nanoparticles during the nucleation burst events, Atmos. Res., accepted, 2005. [6404](#)

5 Vesala, T., Haataja, J., Aalto, P., Altimir, N., Buzorius, G., Garam, E., Hämeri, K., Ilvesniemi, H., Jokinen, V., Keronen, P., Lahti, T., Markkanen, T., Mäkelä, J., Nikinmaa, E., Palmroth, S., Palva, L., Pohja, T., Pumpanen, J., Rannik, U., Siivola, E., Ylitalo, H., Hari, P., and Kulmala, M.: Long-term field measurements of atmosphere-surface interactions in boreal forest combining forest ecology, micrometeorology, aerosol physics and atmospheric chemistry, Trends in Heat, Mass & Momentum Transfer, 4, 17–35, 1998. [6409](#)

10 Weber, R. J., McMurry, P. H., Eisele, F. L., and Tanner, D. J.: Measurements of expected nucleation precursor species and 3–500 nm diameter particles at Mauna Loa observatory, Hawaii, J. Atmos. Sci., 52, 2242–2257, 1995. [6403](#)

15 Weber, R. J., Marti, J., McMurry, P. H., Eisele, F., Tanner, D. J., and Jefferson, A.: Measured atmospheric new particle formation rates: implications for nucleation mechanisms, Chem. Eng. Comm, 151, 53–64, 1996. [6402](#)

Wiedensohler, A.: An approximation of the bipolar charge distribution for particles in the sub-micron range, J. Aerosol Sci., 19, 387–389, 1988. [6403](#), [6406](#), [6407](#)

20 Winklmayr, W., Reischl, G. P., and Lindner, A., and Berner, A.: A new electromobility spectrometer for the measurement of aerosol size distributions in the size range from 1 to 1000 nm, J. Aerosol Sci., 22, 289–296, 1991. [6403](#), [6404](#)

Yu, F. and Turco, R. P.: Ultrafine aerosol formation via ion-mediated nucleation, Geophys. Res. Lett., 27, 883–886, 2000. [6412](#)

**Table 1.** Calculated by using minimum concentration of  $0.1 \text{ cm}^{-3}$ . Exponential fit parameters for event days.  $\text{BSMA} \times 10^{-15}$  shows the slope of BSMA fittings

Date	Negative ions				Positive ions			
	$\beta$	$\lambda$	Eq. (1) @ 1 nm	$\text{BSMA} \times 10^{-15}$	$\beta$	$\lambda$	Eq. (1) @ 1 nm	$\text{BSMA} \times 10^{-15}$
13 April 2005	0.9	2.2	82	–	0.2	0.9	2.3	–
14 April 2005	–0.2	0.0	0.8	4.1	–0.3	0.13	0.6	2.7
16 April 2005	2.1	0.9	14	–	–	–	–	–
17 April 2005	5.4	2.0	300	0.1	–	–	–	0.7
18 April 2005	3.7	1.6	97	–0.1	–	–	–	2.0
19 April 2005	–	–	–	–	–	–	–	–
20 April 2005	0.3	0.4	1.6	–	–	–	–	–
24 April 2005	–	–	–	–	–	–	–	–
25 April 2005	1.0	0.6	4.1	0.2	–	–	–	0.7
26 April 2005	4.3	0.6	17	–0.8	–	–	–	0.2
27 April 2005	3.3	0.5	9.1	0.9	–	–	–	2.5
30 April 2005	–	–	–	2.2	–	–	–	–
02 May 2005	–0.6	0.3	–0.1	4.1	–0.6	0.2	0.1	4.9
03 May 2005	0.7	0.8	4.0	6.9	–0.3	0.0	0.7	6.9
08 May 2005	–	–	–	–0.6	–	–	–	–
10 May 2005	2.2	1.5	46	–0.5	–	–	–	0.0
11 May 2005	3.5	1.5	65	1.7	0.7	0.7	3.8	2.8
12 May 2005	1.7	1.4	27	0.7	0.5	0.6	2.7	0.8
13 May 2005	1.7	1.7	53	–0.6	2.2	1.7	63	–0.2
14 May 2005	0.3	0.9	2.9	–0.5	0.6	0.8	3.6	–1.0
16 May 2005	4.6	1.7	130	–0.2	–	–	–	4.5
17 May 2005	2.6	1.6	67	0.4	0.8	2.6	130	3.8
20 May 2005	0.2	1.9	11	0.0	–0.3	0.2	0.7	0.7
21 May 2005	2.2	1.0	17	2.8	–	–	–	5.8
22 May 2005	1.8	0.4	5.4	0.1	–	–	–	0.3
31 May 2005	–	–	–	0.5	–	–	–	–0.6
01 June 2005	1.0	0.3	3.0	–0.3	–	–	–	0.5
03 June 2005	2.2	0.4	–	–2.2	–	–	–	–6.6
08 June 2005	–	–	–	–0.6	–	–	–	–3.0
09 June 2005	2.7	0.4	7.5	0.1	–	–	–	0.2
10 June 2005	1.3	0.7	6.9	1.8	–	–	–	3.0
11 June 2005	1.1	0.4	3.7	3.1	–	–	–	1.8
15 June 2005	–	–	–	5.1	–	–	–	–0.9
19 June 2005	1.8	0.6	6.3	–0.7	0.4	0.2	–	–3.2
Min	–0.6	0.0	0	–2.2	0.6	0.0	0	–6.6
Max	5.4	2.2	300	6.9	2.2	2.6	130	6.9
Median	1.8	0.8	10	0.2	0.4	0.6	3	0.7
Mean	1.9	1.0	38	1.0	0.4	0.7	21	1.1

## Ion-DMPS

L. Laakso et al.

Title Page

Abstract

Introduction

Conclusions

References

Tables

Figures

◀

▶

◀

▶

Back

Close

Full Screen / Esc

Printer-friendly Version

Interactive Discussion

EGU

## Ion-DMPS

L. Laakso et al.

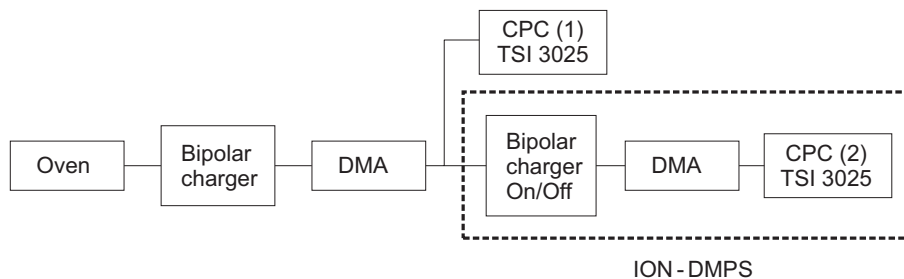


**Fig. 1.** A schematic figure of measurement apparatus and the laboratory setup. In ion-DMPS (boxed with dashed line) ultrafine particles are either directed to the Differential Mobility Analyzer (DMA) via bi-polar charger (Ni-63), where the sample reached an equilibrium charge distribution, or the charger is by-passed and the charge distribution is measured as it is. The DMA has a switchable high voltage supply, which enables measurements of both negative and positive polarities. For laboratory verifications, monomodal test aerosol was produced with a heated oven and directed to the ion-DMPS setup and a reference instrument (TSI model 3025) in order to determine total number concentration of generated aerosol particles and ensure constant output of the generator.

[Title Page](#)[Abstract](#)[Introduction](#)[Conclusions](#)[References](#)[Tables](#)[Figures](#)[◀](#)[▶](#)[◀](#)[▶](#)[Back](#)[Close](#)[Full Screen / Esc](#)[Printer-friendly Version](#)[Interactive Discussion](#)

EGU

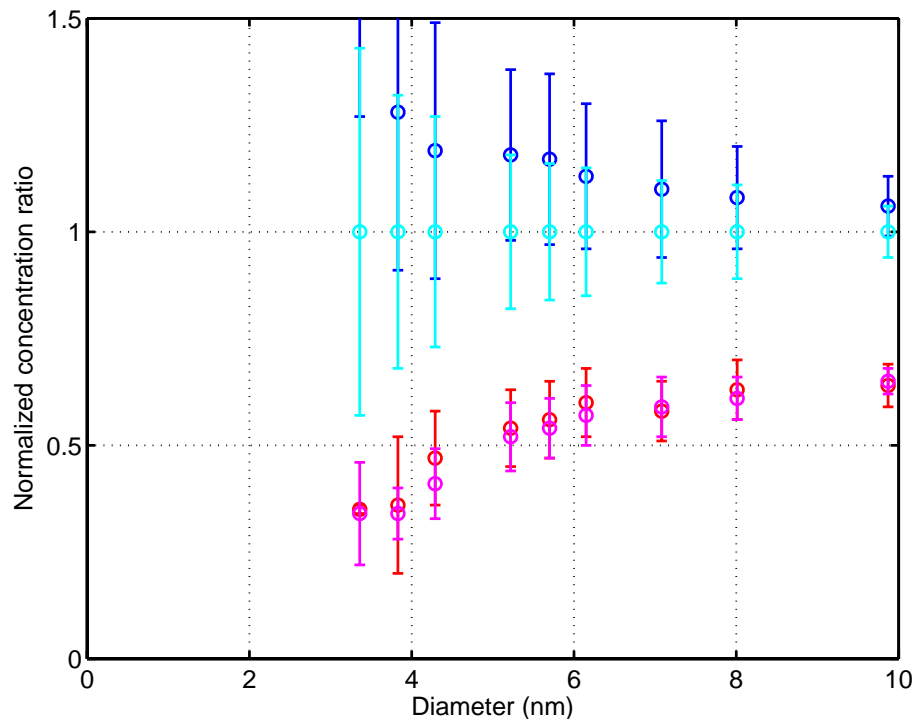


**Fig. 2.** Charge balance of laboratory generated ammonium sulphate (upper panel) and silver (lower panel) particles determined with the Ion-DMPS. Concentration of positive particles detected with the ion-DMPS is lower than negative particles is a result of lower charging efficiency for the positive polarity. In addition, the ratio changes as a function of particle diameter decreases as the diameter decreases. Ratios are normalized with negative concentration. As the charger was turned on, concentrations increased approximately 10%. Colors: dark blue: negative neutralized; Cyan: negative; Magenta: positive; Red: positive neutralized.

[Title Page](#)[Abstract](#)[Introduction](#)[Conclusions](#)[References](#)[Tables](#)[Figures](#)[◀](#)[▶](#)[◀](#)[▶](#)[Back](#)[Close](#)[Full Screen / Esc](#)[Printer-friendly Version](#)[Interactive Discussion](#)

EGU

## Ion-DMPS

L. Laakso et al.

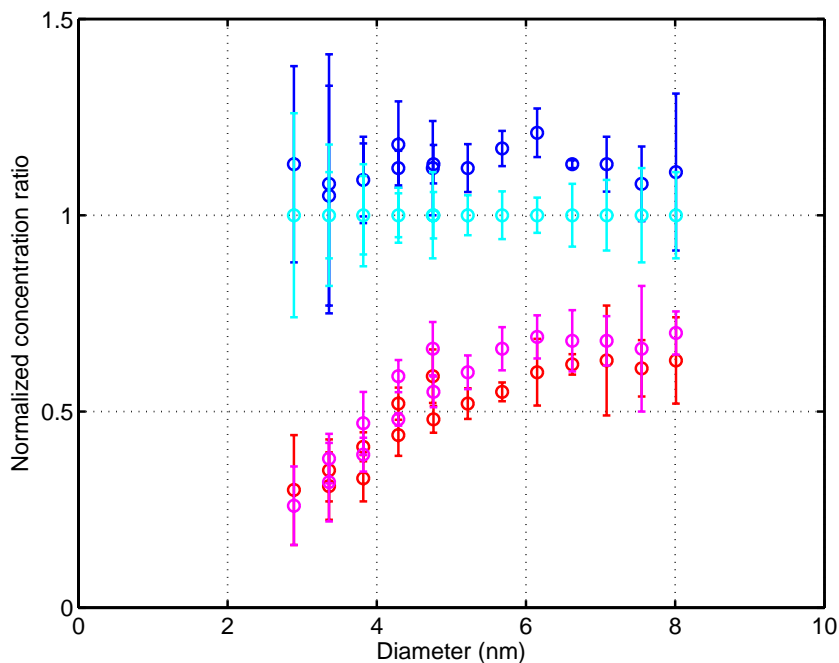


**Fig. 3.** A schematic figure showing the contributions of ion-induced and neutral nucleation. On the left column: absolute concentrations; middle column: charged fraction and equilibrium charged fraction; right column: fraction obtained from ion-DMPS. First row represent situation with pure ion-induced nucleation, second line pure neutral nucleation. Third line is a combination of ion-induced nucleation with a domination of ion nucleation whereas fourth line is a combination of neutral and ion-induced nucleation with dominating neutral nucleation.

[Title Page](#)
[Abstract](#)
[Introduction](#)
[Conclusions](#)
[References](#)
[Tables](#)
[Figures](#)
[◀](#)
[▶](#)
[◀](#)
[▶](#)
[Back](#)
[Close](#)
[Full Screen / Esc](#)
[Printer-friendly Version](#)
[Interactive Discussion](#)

## Ion-DMPS

L. Laakso et al.

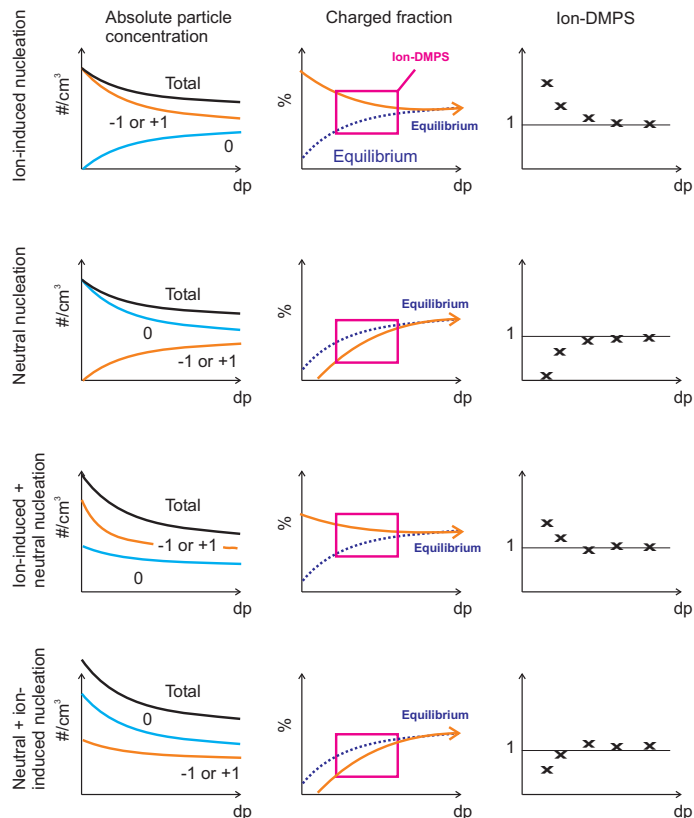


**Fig. 4.** A schematic figure showing the contributions of ion-induced and neutral nucleation. On the left column: absolute concentrations; middle column: charged fraction and equilibrium charged fraction; right column: fraction obtained from ion-DMPS. First row represent situation with pure ion-induced nucleation, second line pure neutral nucleation. Third line is a combination of ion-induced nucleation with a domination of ion nucleation whereas fourth line is a combination of neutral and ion-induced nucleation with dominating neutral nucleation.

Title Page

Abstract

Introduction

Conclusions

References

Tables

Figures

◀

▶

◀

▶

Back

Close

Full Screen / Esc

Printer-friendly Version

Interactive Discussion

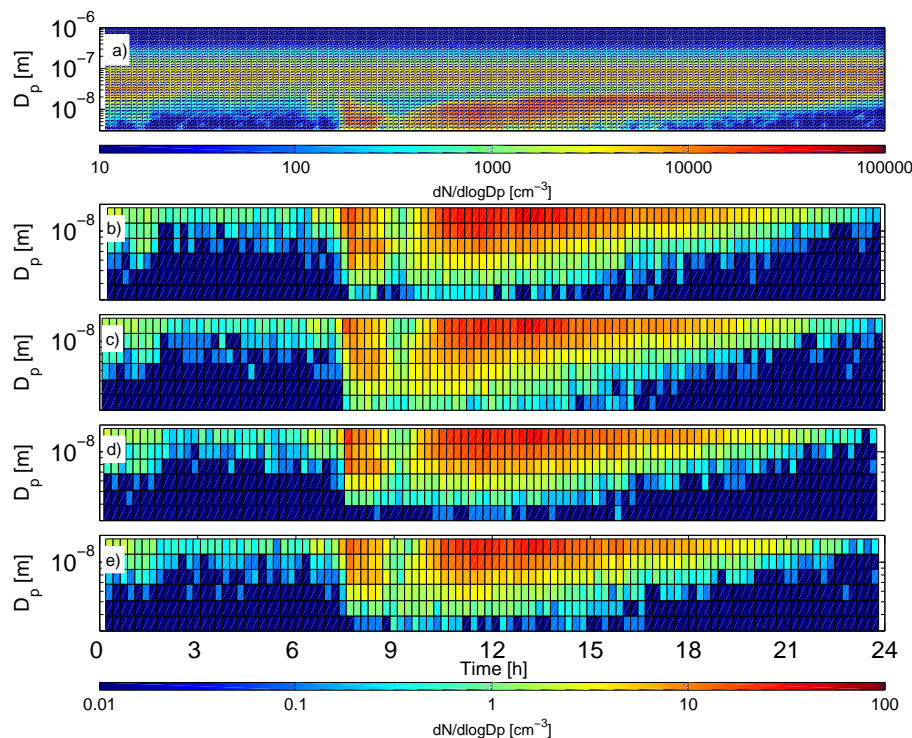


**Fig. 5.** Data on the distribution on the 21 May 2005: **(a)** Size distribution in time of all submicron particles measured with a DMPS, **(b)** size distribution in time of the negative neutralized ions, **(c)** negative natural ions, **(d)** positive neutralized ions, and **(e)** positive natural ions measured with the ion-DMPS. Mind the different scales for concentration and particle diameters in DMPS and ion-DMPS.

[Title Page](#)[Abstract](#)[Introduction](#)[Conclusions](#)[References](#)[Tables](#)[Figures](#)[◀](#)[▶](#)[◀](#)[▶](#)[Back](#)[Close](#)[Full Screen / Esc](#)[Printer-friendly Version](#)[Interactive Discussion](#)

EGU

## Ion-DMPS

L. Laakso et al.

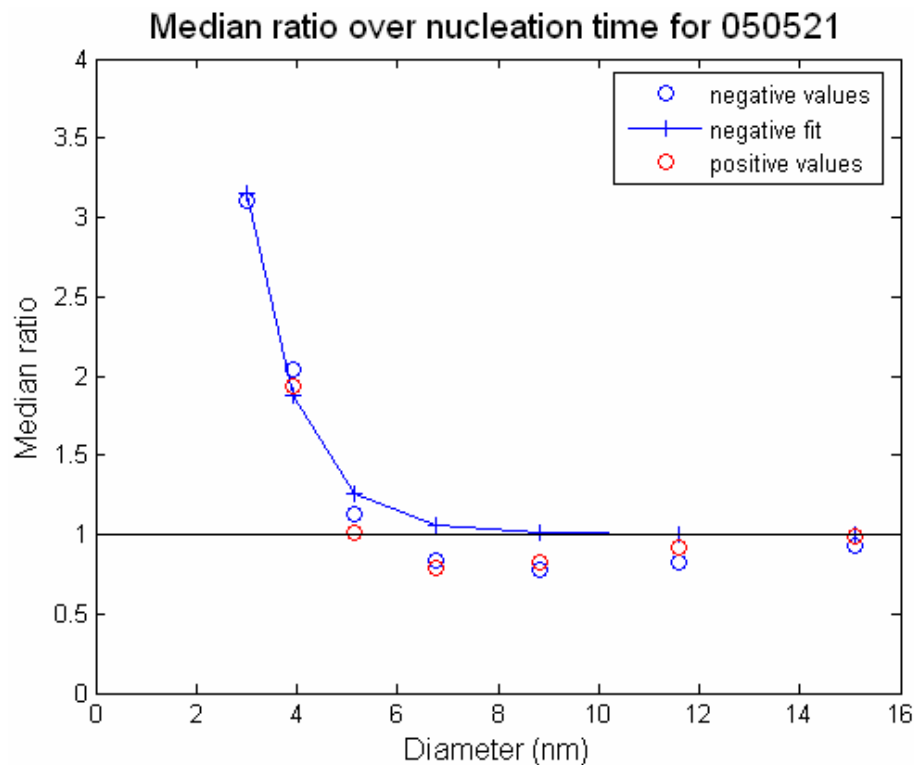


Fig. 6. Day 21 May 2005 – Overcharging occur for both positive and negative ions.

[Title Page](#)[Abstract](#)[Introduction](#)[Conclusions](#)[References](#)[Tables](#)[Figures](#)[◀](#)[▶](#)[◀](#)[▶](#)[Back](#)[Close](#)[Full Screen / Esc](#)[Printer-friendly Version](#)[Interactive Discussion](#)



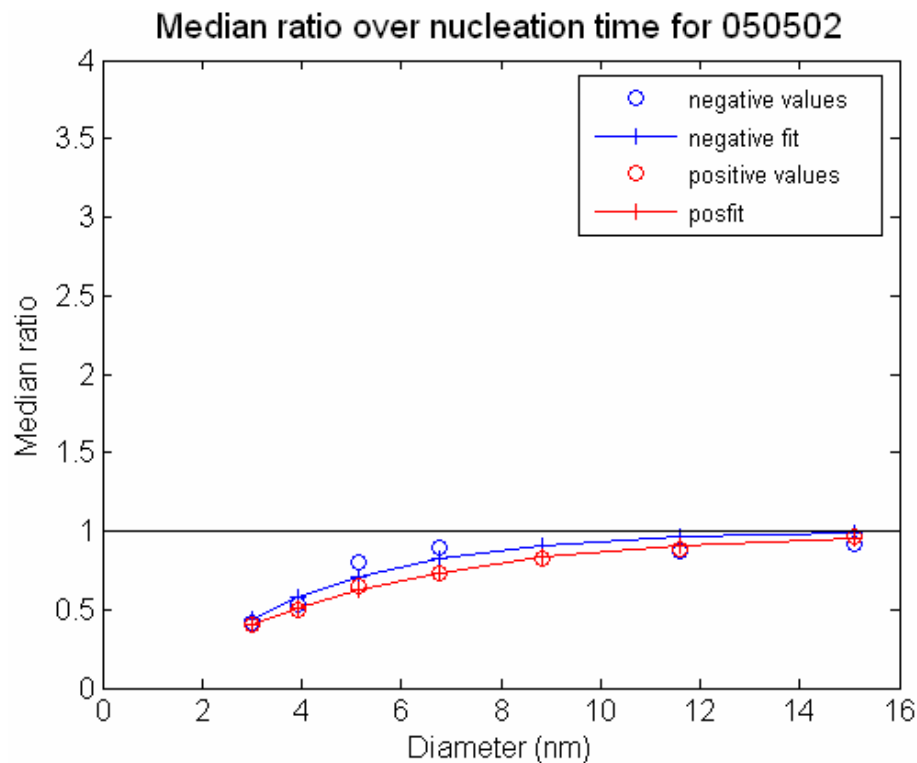
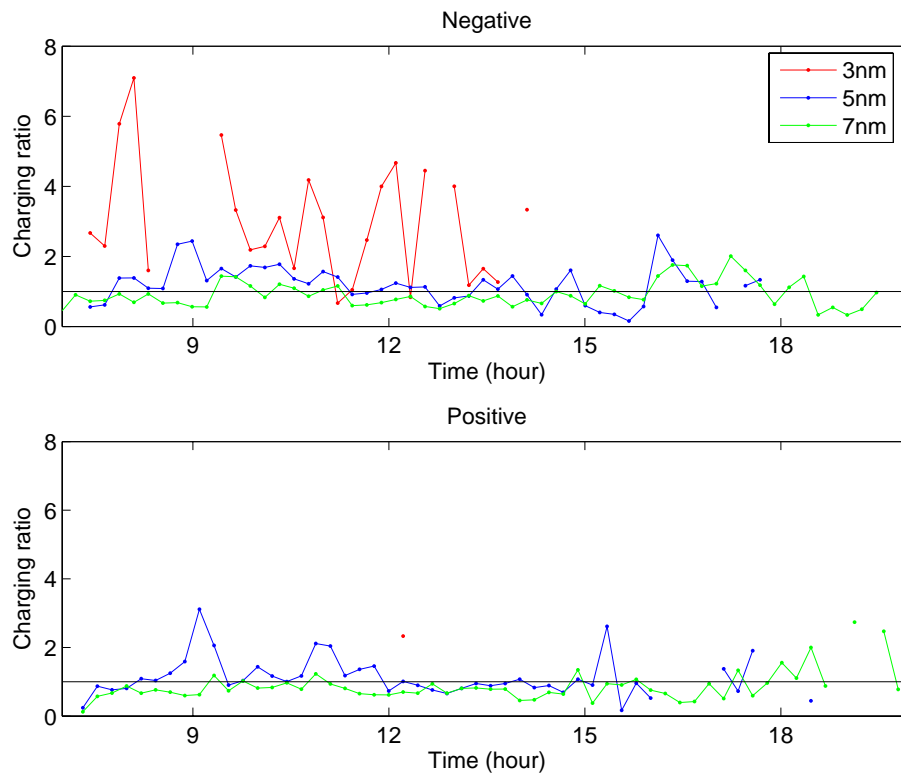


Fig. 7. Day 2 May 2005 – Undercharging occur for both negative and positive ions.

[Title Page](#)[Abstract](#)[Introduction](#)[Conclusions](#)[References](#)[Tables](#)[Figures](#)[◀](#)[▶](#)[◀](#)[▶](#)[Back](#)[Close](#)[Full Screen / Esc](#)[Printer-friendly Version](#)[Interactive Discussion](#)



**Fig. 8.** Time development of charging state during the event day 21 May 2005

[Title Page](#)[Abstract](#)[Introduction](#)[Conclusions](#)[References](#)[Tables](#)[Figures](#)[◀](#)[▶](#)[◀](#)[▶](#)[Back](#)[Close](#)[Full Screen / Esc](#)[Printer-friendly Version](#)[Interactive Discussion](#)

## Ion-DMPS

L. Laakso et al.

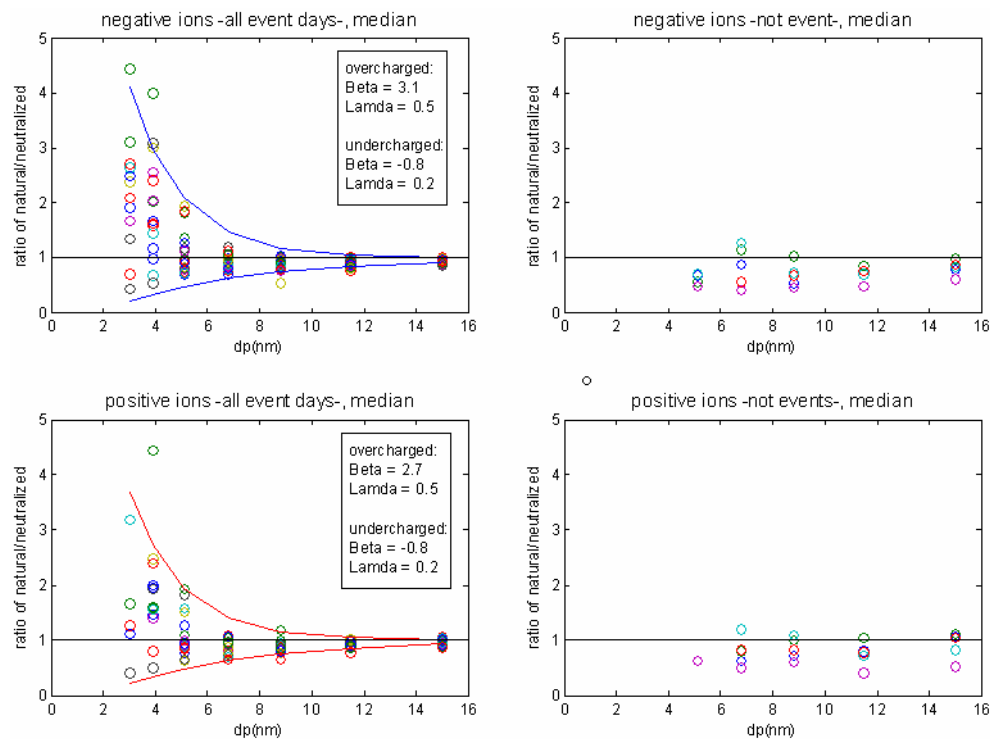


**Fig. 9.** On the left, median ratio for all class 1 and 2 days. On the right, median ratio for a witness sample of 5 non-event days. The upper part is for negative ions while the lower part is for positive ions.

[Title Page](#)
[Abstract](#)
[Introduction](#)
[Conclusions](#)
[References](#)
[Tables](#)
[Figures](#)
[◀](#)
[▶](#)
[◀](#)
[▶](#)
[Back](#)
[Close](#)
[Full Screen / Esc](#)
[Printer-friendly Version](#)
[Interactive Discussion](#)

EGU

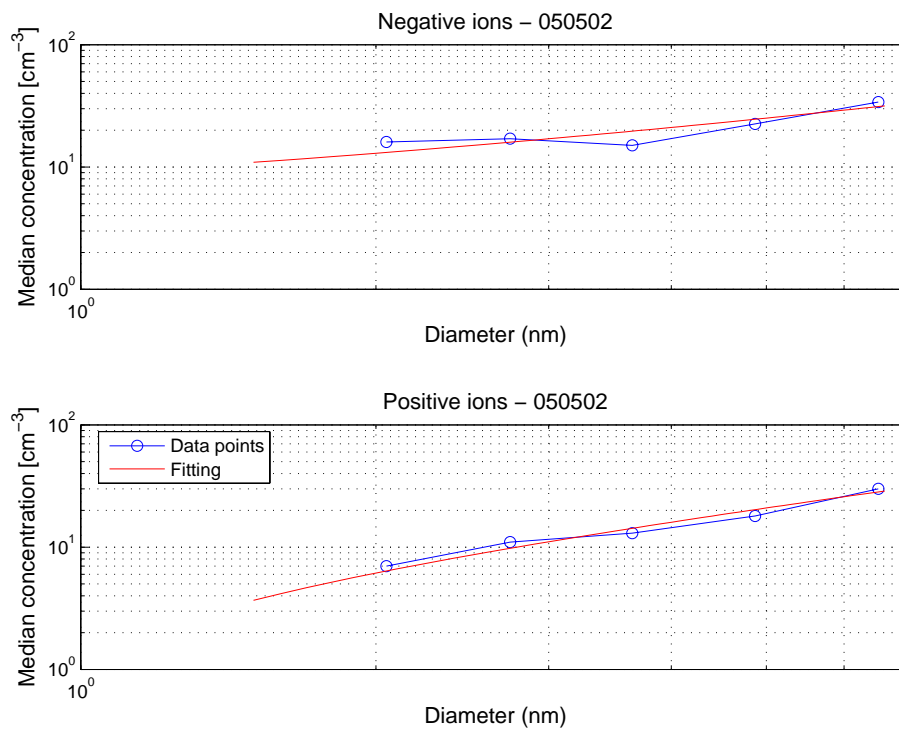


**Fig. 10.** Example of fittings of BSMA concentration data.

[Title Page](#)[Abstract](#)[Introduction](#)[Conclusions](#)[References](#)[Tables](#)[Figures](#)[◀](#)[▶](#)[◀](#)[▶](#)[Back](#)[Close](#)[Full Screen / Esc](#)[Printer-friendly Version](#)[Interactive Discussion](#)

EGU

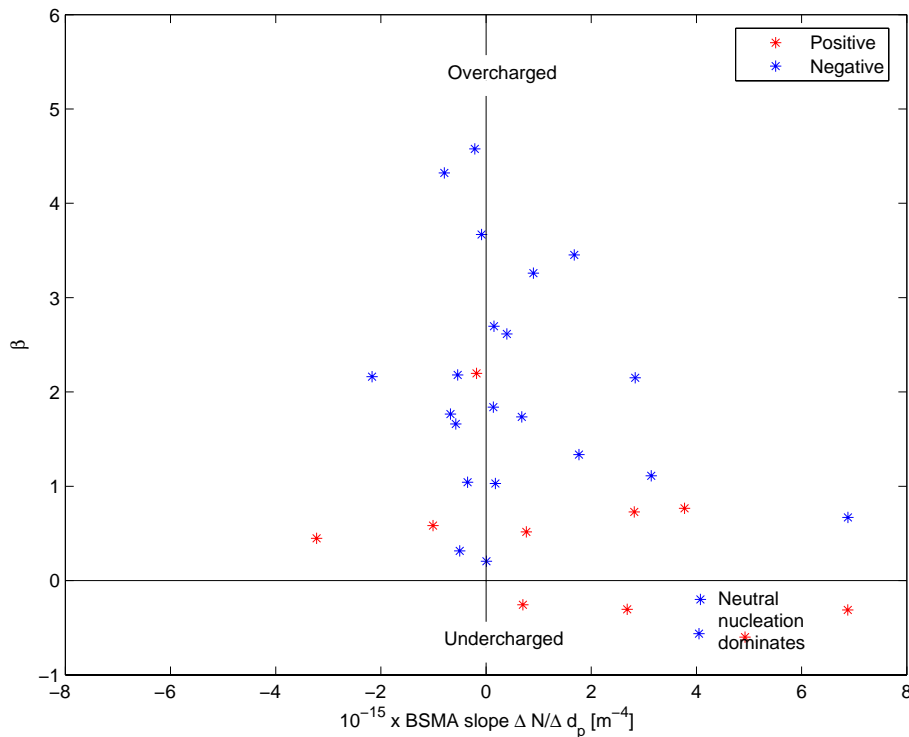


**Fig. 11.** Comparison between BSMA and Ion-DMPS results. x-axis show the slope of fittings done to ion concentrations obtained from BSMA whereas y-axis show the value of Eq. (1). Point with high positive slope and low charged fractions indicate domination of neutral nucleation.

[Title Page](#)
[Abstract](#)
[Introduction](#)
[Conclusions](#)
[References](#)
[Tables](#)
[Figures](#)
[◀](#)
[▶](#)
[◀](#)
[▶](#)
[Back](#)
[Close](#)
[Full Screen / Esc](#)
[Printer-friendly Version](#)
[Interactive Discussion](#)